Synthesis of a Sulfido- and Thiolato-Bridged Trinuclear Bimetallic Cluster $[\{(\eta^5\text{-}C_5Me_5)Ir\}_2\{(\eta^5\text{-}C_5H_5)Ru\}Cl(\mu_3\text{-}S)(\mu_2\text{-}SCH_2CH_2CN)_2]$ and Its Reactions with CO, Isocyanide, and Alkyne

Hidenobu Kajitani, Hidetake Seino, and Yasushi Mizobe*

Institute of Industrial Science, The University of Tokyo, Komaba, Meguro-ku, Tokyo 153-8505, Japan

Received July 22, 2005

Treatment of a sulfido- and thiolato-bridged diiridium complex $[(Cp^*Ir)_2(\mu\text{-}S)(\mu\text{-}SCH_2CH_2CN)_2]$ (**3**; $Cp^* = \eta^5\text{-}C_5Me_5$) with [CpRuCl(tmeda)] ($Cp = \eta^5\text{-}C_5H_5$; tmeda = *N*,*N*,*N*′,*N*′-tetramethylethylenediamine) gave the Ir_2Ru sulfido-thiolato cluster $[(Cp^*Ir)_2(CpRu)Cl(\mu_3\text{-}S)(\mu_2\text{-}SCH_2CH_2CN)_2]$ (**4**), the core structure of which is the same as that of the previously reported Cp*Ru analogue $[(Cp^*Ir)_2(Cp^*Ru)Cl(\mu_3\text{-}S)(\mu_2\text{-}SCH_2CH_2CN)_2]$ (**2**), but the geometry around one Ir atom and the orientation of the cyanoethyl group in one thiolato ligand differ from those in **2**. Cluster **4** reacted with L (L = CO and XyNC; Xy = 2,6-$Me_2C_6H_3$) in the presence of KPF_6 to afford $[(Cp^*Ir)_2(CpRu)(L)(\mu_3\text{-}S)(\mu_2\text{-}SCH_2CH_2CN)_2][PF_6]$ (**5**), in which the ligand L is bonded to one Ir center in a terminal end-on fashion. On the other hand, the reaction of **4** with MeOCOC≡CCOOMe (DMAD) resulted in the insertion of DMAD into the $Ru-S_{sulfido}$ bond, yielding the cluster $[(Cp^*Ir)_2(CpRu)\{\mu_3\text{-}SC(COOMe)=CCOOMe\}(\mu_2\text{-}SCH_2CH_2CN)_2][PF_6]$ (**6**). In **6**, the DMAD molecule bridges the Ru and μ_2-S atoms, and the resulting C=C bond in the DMAD moiety further coordinates to one Ir atom in a side-on manner. To confirm the difference in the reactivities toward alkynes between the Ir sites in **4** and **2**, reaction of DMAD with **2** was carried out, which resulted in the formation of the alkenylthiolato cluster $[(Cp^*Ir)_2(Cp^*Ru)(\mu_3\text{-}S)\{\mu_3\text{-}SC(COOMe)CHCOOMe\}(\mu_2\text{-}SCH_2CH_2CN)][PF_6]$ (**8**) containing the DMAD moiety bonded to the two Ir atoms. Cluster **6** dissolved in MeCN reacted further with CO (10 atm) at 80 °C and XyNC at 60 °C to give $[(Cp^*Ir)_2(CpRu)(L)\{\mu_3\text{-}SC(COOMe)=CCOOMe\}(\mu_2\text{-}SCH_2CH_2CN)_2][PF_6]$ (**9**), where the migration of the DMAD moiety occurred to form the iridathiacyclobutene moiety, accompanied by the coordination of L to the other Ir site. The X-ray analyses have been undertaken to determine the detailed structures for five new clusters: **4**, the BPh_4 analogue of **5b** (L = XyNC) $[(Cp^*Ir)_2(CpRu)(XyNC)(\mu_3\text{-}S)(\mu_2\text{-}SCH_2CH_2CN)_2][BPh_4]$, **6**, **8**, and **9b** (L = XyNC).

Introduction

Sulfur-bridged polynuclear clusters have been attracting much attention because of their relevance to the active sites of metalloenzymes[1] and hydrodesulfurization catalysts.[2] Recent studies in this group have focused on the syntheses of various homo- and heterometallic chalcogenido clusters and clarification of their reactivities toward small molecules.[3] During the course of these studies, we have shown that the hydrosulfido-bridged dinuclear complexes such as $[(Cp^*MCl)_2(\mu\text{-}SH)_2]$ (M = Ru,[4] Ir, Rh;[5,6] $Cp^* = \eta^5\text{-}C_5Me_5$), $[(Cp^*Ir)_2(\mu\text{-}SH)_3]$-Cl (**1**),[6] and $[\{Cp^*Ir(SH)\}_2(\mu\text{-}SH)_2]$[7] are quite versatile precursors for preparing a number of μ-sulfido clusters with the nuclearities ranging from 3 to 7.[3−5,7,8] Complex **1** has also proved to be converted into the μ-sulfido-μ-thiolato cluster $[(Cp^*Ir)_2(Cp^*Ru)Cl(\mu_3\text{-}S)(\mu_2\text{-}SCH_2CH_2CN)_2]$ (**2**)[9] via $[(Cp^*Ir)_2(\mu\text{-}S)(\mu\text{-}SCH_2CH_2CN)_2]$ (**3**).[10] Reactions of **2** with CO, isocyanide, and alkyne have

* To whom correspondence should be addressed. Fax: +81-3-5452-6361. E-mail: ymizobe@iis.u-tokyo.ac.jp.

(1) Lee, S. C.; Holm, R. H. *Chem. Rev.* **2004**, *104*, 1135. (b) Evans, D. J. In *Catalysts for Nitrogen Fixation: Nitrogenases, Relevant Chemical Models, and Commercial Processes*; Smith, B. E., Richards, R. L., Eds.; Kluwer Academic Publishers: Dordrecht, 2004; Chapter 8.

(2) Brorson, M.; King, J. D.; Kiriakidou, K.; Prestopino, F.; Nordlander, E. In *Metal Clusters in Chemistry*; Braunstein, P., Oro, L. A., Raithby, P. R., Eds.; Wiley-VCH: Weinheim, 1999; Chapter 2.6.

(3) (a) Hidai, M.; Mizobe, Y. *Can. J. Chem.* **2005**, *83*, 358. (b) Hidai, M. In *Perspectives in Organometallic Chemistry*; Screttasm C. G., Steele, B. R., Eds.; The Royal Society of Chemistry, 2003; pp 62−73. (c) Hidai, M.; Kuwata, S.; Mizobe, Y. *Acc. Chem. Res.* **2000**, *33*, 46.

(4) Hashizume, K.; Mizobe, Y.; Hidai, M. *Organometallics* **1996**, *15*, 3303.

(5) Tang, Z.; Nomura, Y.; Ishii, Y.; Mizobe, Y.; Hidai, M. *Organometallics* **1997**, *16*, 151.

(6) Tang, Z.; Nomura, Y.; Ishii, Y.; Mizobe, Y.; Hidai, M. *Inorg. Chim. Acta* **1998**, *267*, 73.

(7) Takagi, F.; Seino, H.; Mizobe, Y.; Hidai, M. *Organometallics* **2002**, *21*, 694.

(8) (a) Yeh, W.-Y.; Seino, H.; Amitsuka, T.; Ohba, S.; Hidai, M.; Mizobe, Y. *J. Organomet. Chem.* **2004**, *689*, 2338. (b) Shinozaki, A.; Seino, H.; Hidai, M.; Mizobe, Y. *Organometallics* **2003**, *22*, 4636. (c) Seino, H.; Masumori, T.; Hidai, M.; Mizobe, Y. *Organometallics* **2003**, *22*, 3424. (d) Masui, D.; Kochi, T.; Tang, Z.; Ishii, Y.; Mizobe, Y.; Hidai, M. *J. Organomet. Chem.* **2001**, *620*, 69. (e) Kuwata, S.; Hidai, M. *Coord. Chem. Rev.* **2001**, *213*, 211. See also the references therein.

(9) Takagi, F.; Seino, H.; Hidai, M.; Mizobe, Y. *Organometallics* **2003**, *22*, 1065.

(10) (a) Takagi, F.; Seino, H.; Hidai, M.; Mizobe, Y. *J. Chem. Soc., Dalton Trans.* **2002**, 3603. (b) Takagi, F.; Seino, H.; Hidai, M.; Mizobe, Y. *Can. J. Chem.* **2001**, *79*, 632.

10.1021/om050615a CCC: $30.25
Publication on Web 11/08/2005

Scheme 1

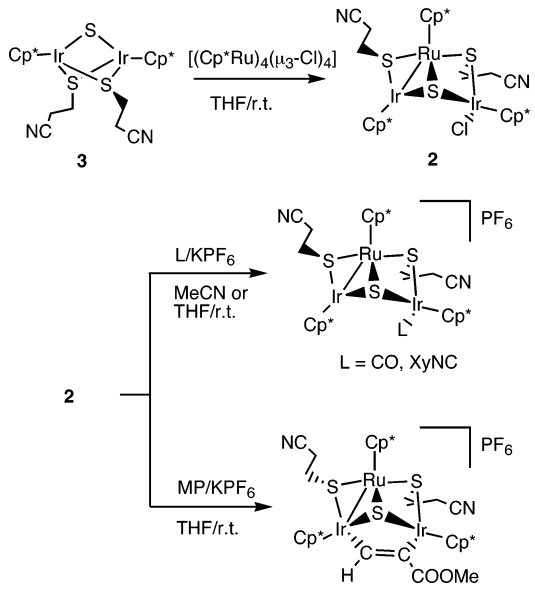

resulted in the incorporation of these molecules to the cluster sites, whereby the former two coordinate to the single Ir site in an end-on fashion and the latter bridges two Ir centers in an η^1:η^1 manner (Scheme 1).[9]

Since even the slight electronic and steric perturbation caused by replacement of the coligands often gives rise to a remarkable change in the reactivities, we have attempted here to prepare the Cp analogue of **2** (Cp = η^5-C_5H_5) by reacting **3** with [CpRuCl(tmeda)] (tmeda = *N,N,N′,N′*-tetramethylethylenediamine) as the Ru^{II} precursor. This has resulted in the isolation of the cluster $[(Cp^*Ir)_2(CpRu)Cl(\mu_3\text{-}S)(\mu_2\text{-}SCH_2CH_2CN)_2]$ (**4**), the metal−sulfur framework of which is essentially the same, but the mutual orientation of the ancillary ligands on one Ir atom and the substituent on one thiolato ligand differs, as compared to those in **2**. Subsequent study on the reactivities of **4** toward CO, isocyanide, and alkyne has demonstrated that the former two also coordinate to one Ir site to afford the CO and isocyanide clusters analogous to those obtained from **2**, whereas the alkyne MeOCOC≡CCOOMe (DMAD) has inserted into the $Ru-S_{sulfido}$ bond and coordinated further to one Ir atom in an η^2 manner at the resulting C=C unit to give the alkyne-incorporating cluster of a novel type. In this paper, we wish to describe the details of these new mixed-metal−sulfur clusters together with the cluster derived from DMAD and **2**.

Results and Discussion

Synthesis and Structure of the Ir_2Ru Sulfido-Thiolato Cluster 4. Treatment of **3** with [CpRuCl(tmeda)] in THF at room temperature afforded the Ir_2Ru trinuclear sulfido-thiolato cluster **4** in 62% yield (eq 1), the structure of which has been determined unambiguously by an X-ray analysis, as depicted in Figure 1. Cluster **4** has a nonsymmetrical triangular core with one μ_3-sulfido ligand, two μ_2-thiolato ligands bridging the Ir−Ru edges, and one Cl ligand bonded to one Ir center. These structural features for **4** are the same as those for **2**. However, the orientation of the cyanoethyl group in the thiolato ligand bound to the nonbonded Ir−Ru edge and the geometry around Ir(2) differ from each other.

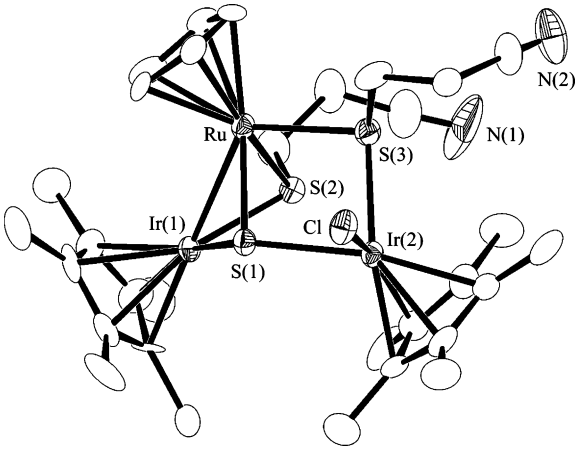

Figure 1. ORTEP drawing of **4** at the 30% probability level. Hydrogen atoms are omitted for clarity.

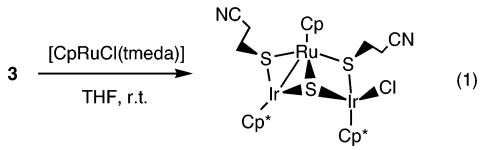

For the Ir_2Ru triangle, the Ir(1)−Ru distance at 2.761(1) Å is indicative of the presence of a metal−metal single bond, whereas the separation between Ir(2) and Ru (3.648(1) Å) suggests the absence of any bonding interaction between these two atoms. Indeed, by assuming the presence of a dative bond from Ru to Ir(1), electron counts around the two Ir^{III} and one Ru^{II} center all satisfy the EAN rule. The Ir(1)−Ru bond length in **4** is significantly shorter than that in **2** at 2.8362(5) Å, despite the weaker electron-donating ability of the Cp ligand than the Cp* ligand. This shortening is presumably interpreted in terms of the decrease in the steric repulsion between the CpRu and Cp*Ir units in **4**, as compared to that between the Cp*Ru and Cp*Ir moieties in **2**.

The Ir(2)−S(1)−Ru−S(3) torsion angle of only 8.6(2)° indicates that these four atoms are almost coplanar. With respect to this plane, the Cp and Cp* ligands are mutually anti and the cyanoethyl group and the Cl ligand are both pointed toward the direction opposite the Cp*Ir(1) fragment. These present a sharp contrast to the geometry around the corresponding $IrRuS_2$ plane in **2** with the two mutually syn Cp* ligands together with the cyanoethyl group and the Cl ligand oriented in the endo direction of the cluster core.

The ^{1}H NMR spectrum of **4** is consistent with the X-ray structure, exhibiting three singlets at δ 1.46, 1.55, and 4.18 assignable to two Cp* and Cp ligands, respectively, together with the signals due to the methylene protons of the cyanoethyl groups, while the IR spectrum shows the characteristic ν(C≡N) band at 2245 cm^{-1}.

Reactions of 4 with CO and Isocyanide. As observed for **2**, reactions of **4** with CO (1 atm) and a slightly excess amount of XyNC (Xy = 2,6-$Me_2C_6H_3$) in THF at room temperature in the presence of KPF_6 afforded the cationic clusters $[(Cp^*Ir)_2(CpRu)(L)(\mu_3\text{-}S)(\mu_2\text{-}SCH_2CH_2CN)_2][PF_6]$ (**5a**: L = CO, **5b**: L = XyNC)

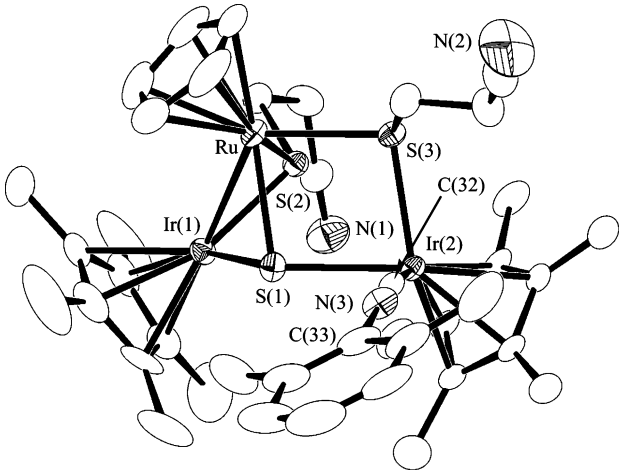

Figure 2. ORTEP drawing of the cation in **5b′** at the 30% probability level. Hydrogen atoms are omitted for clarity.

Table 1. Selected Interatomic Distances (Å) and Angles (deg) in 4

(a) Distances			
Ir(1)−Ru	2.761(1)	Ir(1)···Ir(2)	4.1852(9)
Ir(2)···Ru	3.648(1)		
Ir(1)−S(1)	2.311(4)	Ir(1)−S(2)	2.307(4)
Ir(2)−S(1)	2.398(4)	Ir(2)−S(3)	2.392(4)
Ir(2)−Cl	2.415(4)	Ru−S(1)	2.382(4)
Ru−S(2)	2.355(4)	Ru−S(3)	2.410(4)
(b) Angles			
S(1)−Ir(1)−S(2)	82.5(1)	S(1)−Ir(2)−S(3)	80.3(1)
S(1)−Ir(2)−Cl	85.6(1)	S(3)−Ir(2)−Cl	92.1(1)
S(1)−Ru−S(2)	80.0(1)	S(1)−Ru−S(3)	80.2(1)
S(2)−Ru−S(3)	80.5(1)		
Ir(1)−S(1)−Ir(2)	125.4(2)	Ir(1)−S(1)−Ru	72.1(1)
Ir(2)−S(1)−Ru	99.5(1)	Ir(1)−S(2)−Ru	72.6(1)
Ir(2)−S(3)−Ru	98.9(2)		

in moderate yields (eq 2). Treatment with excess XyNC also gave the monoisocyanide cluster **5b** exclusively. Replacement of the Cl ligand by L did not take place in the absence of KPF_6. The structure of **5** has been determined by X-ray crystallography using a single crystal of $[(Cp^*Ir)_2(CpRu)(CNXy)(\mu_3\text{-}S)(\mu_2\text{-}SCH_2CH_2CN)_2][BPh_4]$ (**5b′**), which was obtained by analogous treatment of **4** with XyNC but by using $NaBPh_4$ in place of KPF_6. Figure 2 shows the X-ray structure of the cation in **5b′**, demonstrating unambiguously that the substitution of the Cl ligand by XyNC proceeds with retention of both the cluster core structure and the geometries around all metal centers. Metrical parameters associated with three metals and three S atoms are listed in Table 2 and are in good agreement or almost comparable with those in **4**.

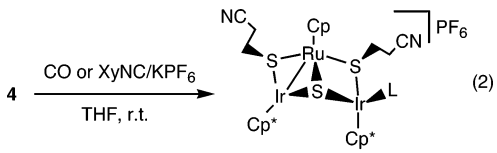

5a: L = CO; **5b**: L = XyNC

The IR spectrum of **5a** exhibits a strong ν(C≡O) band at 2021 cm^{-1}, while that of **5b** shows an intense band assignable to ν(N≡C) at 2125 cm^{-1}. Analogous CO and XyNC clusters derived from **2** show these bands at 2020 and 2114 cm^{-1}, respectively.[9] Thus, replacement of the Cp*Ru fragment by the CpRu moiety causes only a little

Table 2. Selected Interatomic Distances (Å) and Angles (deg) in 5b′

(a) Distances			
Ir(1)−Ru	2.7814(5)	Ir(1)···Ir(2)	4.1827(4)
Ir(2)···Ru	3.6427(4)		
Ir(1)−S(1)	2.295(1)	Ir(1)−S(2)	2.291(1)
Ir(2)−S(1)	2.414(1)	Ir(2)−S(3)	2.377(1)
Ir(2)−C(32)	1.908(5)	Ru−S(1)	2.383(1)
Ru−S(2)	2.374(1)	Ru−S(3)	2.414(1)
N(3)−C(32)	1.167(6)		
(b) Angles			
S(1)−Ir(1)−S(2)	85.38(4)	S(1)−Ir(2)−S(3)	80.71(5)
S(1)−Ir(2)−C(32)	82.3(2)	S(3)−Ir(2)−C(32)	97.0(2)
S(1)−Ru−S(2)	81.61(4)	S(1)−Ru−S(3)	80.56(5)
S(2)−Ru−S(3)	82.79(4)		
Ir(1)−S(1)−Ir(2)	125.30(6)	Ir(1)−S(1)−Ru	72.93(4)
Ir(2)−S(1)−Ru	98.81(5)	Ir(1)−S(2)−Ru	73.17(4)
Ir(2)−S(3)−Ru	98.97(5)		
Ir(2)−C(32)−N(3)	173.1(5)	C(32)−N(3)−C(33)	164.8(6)

change in the electron-donating ability of this Ir site, if any. The ν(C≡O) values reported previously for the related Cp*Ir-sulfur complexes are, for example, 1994, 2040, and 1974 cm^{-1} for $[Cp^*Ir(SPh)_2(CO)]$,[11] $[Cp^*Ir(SC_6F_5)_2(CO)]$,[12] and $[\{Cp^*Ir(CO)\}_2(\mu\text{-}S)_2]$,[13] respectively. With respect to the XyNC complexes, the Cp*Ir complexes with sulfur coligands are not precedented, but the ν(N≡C) bands of $[Cp^*IrI_2(CNXy)]$,[14] $[Cp^*IrCl\{PPh_2(C_6H_3(OMe)_2)\}(CNXy)][PF_6]$,[15] and $[\{Cp^*Ir(CNXy)\}_2(\mu\text{-}Ph_2PC_{10}H_6PPh_2)][OTf]_2$[16] are 2140, 2160, and 2155 cm^{-1}.

Reactions of 4 with Alkynes. As described above, when **2** was treated with methyl propiolate (MP) in the presence of KPF_6, the cluster containing the alkyne bound to the two Ir atoms in an η^1:η^1 mode was isolated (Scheme 1). On the other hand, similar treatment of **4** with MP has turned out to proceed in a more complex manner. Thus, the NMR spectrum of the reaction mixture indicated the presence of at least two major products in which MP was incorporated. However, since we could not isolate any products in a pure form or as single crystals from this mixture, characterization of these alkyne clusters was unsuccessful.

Now, it has been found that when **4** was allowed to react with DMAD in THF at room temperature in the presence of KPF_6, $[(Cp^*Ir)_2(CpRu)\{\mu_3\text{-}SC(COOMe)=CCOOMe\}(\mu_2\text{-}SCH_2CH_2CN)_2][PF_6]$ (**6**) was obtained in satisfactory yield after the crystallization of the reaction product from MeCN−ether (eq 3). Cluster **6** has been characterized by an X-ray analysis; the structure of the cation in **6** is shown in Figure 3, while the selected interatomic distances and angles therein are listed in Table 3.

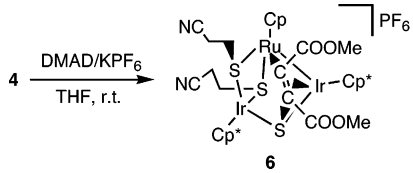

6

Cluster **6** consists of the DMAD molecule inserted into the $Ru-S_{sulfido}$ bond in **4**, which coordinates further to one Ir atom in an η^2 manner at the resultant C=C

(11) Herberhold, M.; Jin, G.; Rheingold, A. L. *J. Organomet. Chem.* **1998**, *570*, 241.
(12) Andrade, J.; Garcia, J. J.; Torrens, H.; Rio, F.; Claver, C.; Ruiz, N. *Inorg. Chim. Acta* **1997**, *255*, 389.

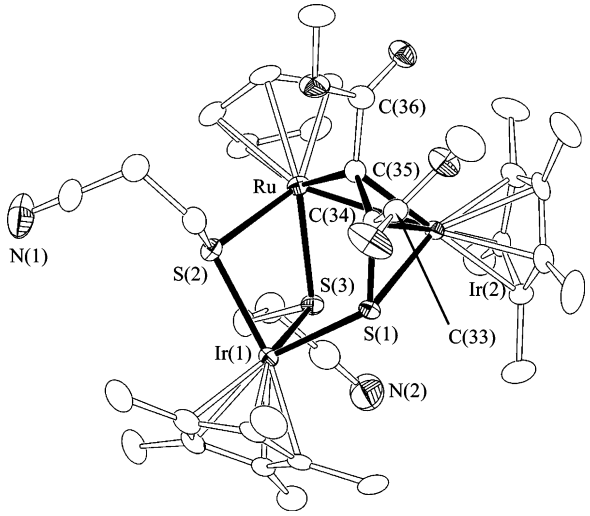

Figure 3. ORTEP drawing of the cation in **6** at the 30% probability level. Hydrogen atoms are omitted for clarity.

Table 3. Selected Interatomic Distances (Å) and Angles (deg) in 6

(a) Distances			
Ir(1)···Ru	3.5926(6)	Ir(1)···Ir(2)	4.0137(4)
Ir(2)−Ru	2.8631(6)		
Ir(1)−S(1)	2.318(2)	Ir(1)−S(2)	2.346(2)
Ir(1)−S(3)	2.383(2)	Ir(2)−S(1)	2.350(2)
Ir(2)−C(34)	2.156(6)	Ir(2)−C(35)	2.085(7)
Ru−S(2)	2.394(2)	Ru−S(3)	2.424(2)
Ru−C(35)	2.079(7)	S(1)−C(34)	1.780(7)
C(34)−C(35)	1.401(8)		
(b) Angles			
S(1)−Ir(1)−S(2)	92.55(6)	S(1)−Ir(1)−S(3)	82.42(6)
S(2)−Ir(1)−S(3)	76.39(6)	Ru−Ir(2)−S(1)	84.02(4)
Ir(2)−Ru−S(2)	108.19(4)	Ir(2)−Ru−C(35)	46.5(2)
S(2)−Ru−S(3)	74.71(6)	S(3)−Ru−C(35)	109.0(2)
Ir(1)−S(1)−Ir(2)	118.59(6)	Ir(1)−S(1)−C(34)	121.3(2)
Ir(2)−S(1)−C(34)	61.1(2)	Ir(1)−S(2)−Ru	98.57(6)
Ir(1)−S(3)−Ru	96.72(6)		
Ir(2)−C(34)−S(1)	72.6(2)	Ir(2)−C(34)−C(33)	130.3(5)
Ir(2)−C(34)−C(35)	68.0(4)	S(1)−C(34)−C(33)	115.2(5)
S(1)−C(34)−C(35)	117.8(5)	C(33)−C(34)−C(35)	127.0(7)
Ir(2)−C(35)−Ru	86.9(3)	Ir(2)−C(35)−C(34)	73.5(4)
Ir(2)−C(35)−C(36)	125.9(5)	Ru−C(35)−C(34)	126.6(5)
Ru−C(35)−C(36)	116.2(4)	C(34)−C(35)−−C(36)	115.5(6)

moiety (Ir(2)−C(34): 2.156(6) Å, Ir(2)−C(35): 2.085(7) Å). This Ir atom is connected directly to the Ru atom by the Ir−Ru single bond with a distance of 2.8631(6) Å. Concomitant migration of the μ-thiolato ligand takes place from this Ir center to the other, yielding the Ir-(μ-$SCH_2CH_2CN)_2$Ru fragment without a metal−metal bond, where the configuration of the two cyanoethyl groups is anti.

For the Ru−C(35)═C(34)−S(1) linkage, the C(34)−C(35) bond length at 1.401(8) Å is intermediate between the typical C−C single and double-bond distances and comparable to those in the π-bonded alkenethiolato ligands in, for example, $[Cp^*Ir\{\mu,\eta^3$-SC(Me)═$CHCH_2$-COMe$\}]_2[BF_4]_2$[17] (1.392(9) Å) and $[(Cp^*Ru)_2(CpTi)_2Pd_2$-$(PPh_3)(\mu_3$-$S)_3(\mu_2$-O)$\{\mu_3$-SC(COOMe)═CCOOMe$\}]$ (**7**; 1.401-(9) Å).[18] The Ru−C(35) and S(1)−C(34) distances of 2.082(9) and 1.78(1) Å in **6** are not exceptional; neither are those for the Ru−C and S−C single bonds. The four C atoms C(33)−C(36) from DMAD as well as the S(1) atom are almost coplanar (torsion angles: C(33)−C(34)−C(35)−C(36) = 1(1)°, S(1)−C(34)−C(35)−C(36) = −177.9(7)°), and the Ru atom is slightly out of this plane with a S(1)−C(34)−C(35)−Ru angle of 18(1)°. The sums of the three bond angles around C(34) and C(35) associated with these six atoms are 360° and 358°, respectively, indicating that these C atoms are essentially of sp^2 character.

The NMR data for **6** are consistent with this solid-state structure. Thus, as for the incorporated DMAD, the methoxy protons are observed as two singlets at δ 3.71 and 3.79 in its ^{1}H NMR spectrum, while the signals due to the C(34) and C(35) atoms appear at δ 70.6 and 158.5 in its $^{13}C\{^1H\}$ NMR spectrum.

It is to be noted that insertion of alkynes into the M−μ_3-S bond has been rarely observed: the precedented examples are **7** obtained from the reaction of $[(Cp^*Ru)_2(CpTi)_2Pd_2(PPh_3)(\mu_3$-$S)_4(\mu_3$-$O)(\mu$-$H)_2]$ with DMAD[18] and $[Cp^*MFe_3(\mu_3$-$S)\{\mu_3$-CH═C(R)S$\}(CO)_6(\mu_3$-CCPh)] (M = Mo, W; R = Ph, ^{n}Bu) or $[Cp^*MFe_3(\mu_3$-$S)$-$\{\mu_3$-CFC═C(H)S$\}(CO)_7(\mu_3$-CCPh)] (M = Mo, W) from $Fe_3S_2(CO)_9$, Cp*M(C≡CPh), and HC≡CR (R = Ph, ^{n}Bu, Fc; Fc = ferrocenyl).[19] A related structure has also been demonstrated for the μ_4-SCR═CR′ ligand in $[Os_4(CO)_{12}$-(μ_4-SCPh═CH)] prepared from $[Os_4(CO)_{12}(\mu_3$-S)] and HC≡CPh,[20] and that in $[Ru_4(CO)_{12}(\mu_4$-SC═CCH_2CMe-^{t}Bu)] from $[Ru_3(CO)_{12}]$ and phenylthiocyclobutene PhSC═$CHCH_2C(Me)^tBu$.[21] On the other hand, the μ_2-SCR═CR′ ligands, which are generated from sulfide[22] or thiolate[23] with alkyne, or from thioether,[24] are more ubiquitous.

Conversion of **4** into **6** is presumably initiated by the formation of the π-DMAD complex **i**, as observed in the reactions with CO and XyNC to give **5**, but then the alkyne in **i** might interact with the sulfido ligand and the Ru atom to give the intermediates **ii** and then **iii** (Scheme 2). This presents a sharp contrast to the reaction of **2** with MP previously reported, where the MP molecule, being bound at first similarly to the Ir center, subsequently bridges two Ir atoms. This difference in the reaction courses probably arises from the geometry around the Ir atoms; namely, in **i**, the DMAD molecule is ligating to the Ir atom from the direction opposite that of MP in **2**. Hence, the DMAD ligand incorporated into **4** is unable to interact with the other Cp*Ir site but can bind readily to the sulfide, which leads to the formation of the possible intermediates **ii** and **iii**.

(13) Dobbs, D. A.; Bergman, R. G. *Inorg. Chem.* **1994**, *33*, 5329.
(14) Jones, W. D.; Duttweiler, R. P., Jr.; Feher, F. J. *Inorg. Chem.* **1990**, *29*, 1505.
(15) Yamamoto, Y.; Kawasaki, K.; Nishimura, S. *J. Organomet. Chem.* **1999**, *587*, 49.
(16) Yamamoto, Y.; Miyauchi, F. *Inorg. Chim. Acta* **2002**, *334*, 77.
(17) Paz-Sandoval, M. A.; Cervantes-Vasquez, M.; Young, V. G., Jr.; Guzei, I. A.; Angelici, R. *Organomeallics* **2004**, *23*, 1274.
(18) Kuwata, S.; Kabashima, S.; Ishii, Y.; Hidai, M. *J. Am. Chem. Soc.* **2001**, *123*, 3826.
(19) Mathur, P.; Bhunia, A. K.; Srinivasu, C.; Mobin, S. M. *J. Organomet. Chem.* **2003**, *670*, 144.
(20) Adams, R. D.; Wang, S. *Organometallics* **1985**, *4*, 1902.
(21) Adams, R. D.; Qu, X.; Wang, S. *Organometallics* **1994**, *13*, 1272.
(22) (a) Adams, R. D.; Wang, S. *Organometallics* **1987**, *6*, 739. (b) Ikada, T.; Mizobe, Y.; Hidai, M. *Organometallics* **2001**, *20*, 4441.
(23) (a) Fässler, Th.; Huttner, G. *J. Organomet. Chem.* **1989**, *376*, 367. (b) Fässler, Th.; Huttner, G.; Günauer, D.; Fiedler, S.; Eber, B. *J. Organomet. Chem.* **1990**, *381*, 409. (c) Robin, F.; Rumin, R.; Talarmin, J.; Petillon, F. Y.; Muir, K. W. *Organometallics* **1993**, *12*, 365. (d) Hogarth, G.; O'Brien, M.; Tocher, D. A. *J. Organomet. Chem.* **2003**, *672*, 22.
(24) (a) Schrauzer, G. N.; Rabinowitz, H. N.; Frank, J. A. K.; Paul, I. C. *J. Am. Chem. Soc.* **1970**, *92*, 212. (b) Rumin, R.; Pétillon, F. *Organometallics* **1990**, *9*, 944. (c) Rumin, R.; Pétillon, F. Y.; Henderson, A. H.; Manojlovic-Muir, L.; Muir, K. W. *J. Organomet. Chem.* **1987**, *336*, C50.

Scheme 2

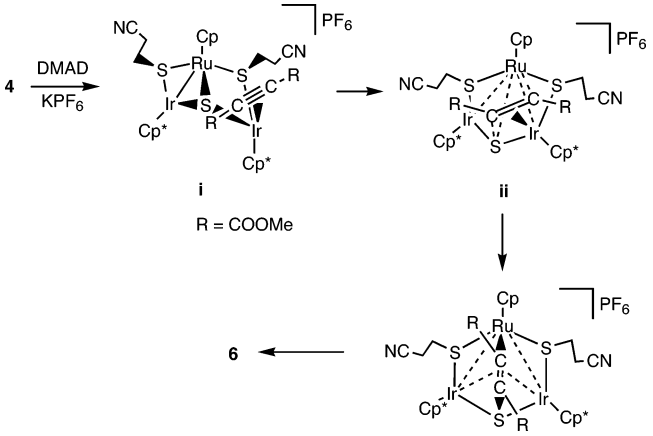

Table 4. Selected Interatomic Distances (Å) and Angles (deg) in 8

(a) Distances

Ir(1)−Ru	2.767(1)	Ir(1)···Ir(2)	3.9281(7)
Ir(2)···Ru	3.5690(8)		
Ir(1)−S(1)	2.355(4)	Ir(1)−S(2)	2.308(3)
Ir(1)−C(37)	2.131(9)	Ir(2)−S(1)	2.288(2)
Ir(2)−S(3)	2.369(3)	Ir(2)−C(36)	2.09(1)
Ru−S(1)	2.301(3)	Ru−S(2)	2.275(4)
Ru−S(3)	2.384(3)	S(3)−C(36)	1.80(1)
C(36)−C(37)	1.51(2)		

(b) Angles

S(1)−Ir(1)−S(2)	104.4(1)	S(1)−Ir(1)−C(37)	83.0(4)
S(2)−Ir(1)−C(37)	95.4(3)	S(1)−Ir(2)−S(3)	78.32(9)
S(1)−Ir(2)−C(36)	84.2(3)	S(3)−Ir(2)−C(36)	47.1(4)
S(1)−Ru−S(2)	107.2(1)	S(1)−Ru−S(3)	77.76(9)
S(2)−Ru−S(3)	91.9(1)	Ir(1)−S(1)−Ir(2)	115.5(1)
Ir(1)−S(1)−Ru	72.92(9)	Ir(2)−S(1)−Ru	102.1(1)
Ir(1)−S(2)−Ru	74.27(9)	Ir(2)−S(3)−Ru	97.3(1)
Ir(2)−S(3)−C(36)	58.2(4)	Ru−S(3)−C(36)	109.7(3)
Ir(2)−C(36)−S(3)	74.8(5)	Ir(2)−C(36)−C(37)	117.7(7)
Ir(2)−C(36)−C(35)	110.6(7)	S(3)−C(36)−C(37)	123.0(7)
S(3)−C(36)−C(35)	110.1(9)	C(35)−C(36)−C(37)	114(1)
Ir(1)−C(37)−C(36)	117(1)	Ir(1)−C(37)−C(38)	114.8(7)
C(36)−C(37)−C(38)	109.6(9)		

To confirm this difference in the reactivities toward alkynes between the Ir sites in **4** and **2**, the reaction of DMAD with **2** has also been investigated, since that of MP with **4** is ellusive, as described already.

Reaction of 2 with DMAD. It has turned out that by treatment of **2** with DMAD in THF at room temperature in the presence of KPF_6, an alkenylthiolato cluster

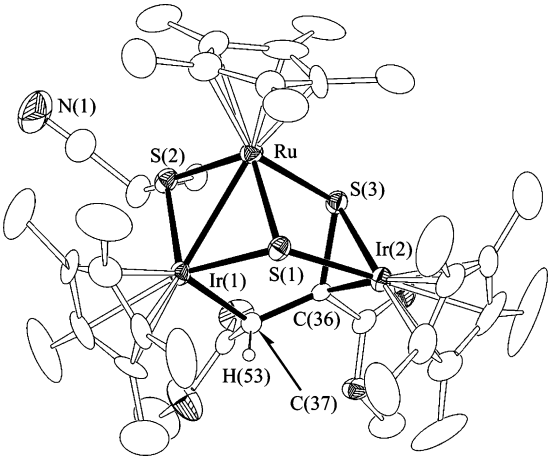

Figure 4. ORTEP drawing of the cation in **8** at the 30% probability level. Hydrogen atoms except for H(53) are omitted for clarity.

$[(Cp^*Ir)_2(Cp^*Ru)(\mu_3\text{-}S)\{\mu_3\text{-}SC(COOMe)\text{-}CHCOOMe\}(\mu_2\text{-}SCH_2CH_2CN)][PF_6]$ (**8**) can be obtained in moderate yield (eq 4). The structure of **8** has been characterized in detail by the X-ray analysis, as shown in Figure 4, and the important metrical parameters for **8** are listed in Table 4. Cluster **8** has the μ_3-alkenylthiolato ligand, in which the S atom binds to the Ru and one Ir atom in a μ_2-manner and the alkenyl moiety bridges the two Ir atoms in a $\mu^2{:}\eta^1{:}\eta^1$ fashion. This ligand might be produced formally by the addition of DMAD to the hydrosulfido group generated in situ from the cyanoethylthiolato ligand through the elimination of $CH_2{=}CHCN$, but the actual mechanism is unknown. Nevertheless, it has been clearly shown as expected that the DMAD moiety is incorporated into the cluster as the bridge between two Ir atoms, and this observation about the reactivity of **2** is consistent with the reaction of MP with **2**.

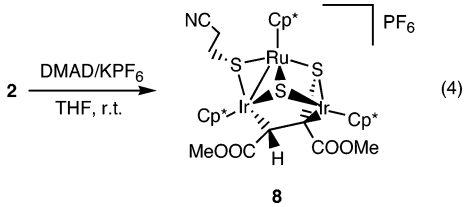

(4)

Cluster **8** has a triangular Ir_2Ru core bridged by one μ_3-sufido and two μ_2-thiolato ligands. One metal−metal bond is present between Ru and Ir(1), the distance of which is 2.767(1) Å. The C(36)−C(37) bond length of 1.51(2) Å falls in the range of the C−C single bond distances, and the J_{C-H} value observed between the C(37) and H(53) atoms in the ^{13}C NMR spectrum is also diagnostic of the sp^3 character for this C atom.

Reactions of 6 with CO and Isocyanide. Although **6** is unreactive toward CO or isocyanide under ambient conditions, it did react under more forcing conditions. Thus, **6** dissolved in MeCN was allowed to react with CO gas (10 atm) at 80 °C, and the monocarbonyl cluster $[(Cp^*Ir)_2(CpRu)(CO)\{\mu_3\text{-}SC(COOMe){=}CCOOMe\}(\mu_2\text{-}SCH_2CH_2CN)_2][PF_6]$ (**9a**) was obtained in 60% yield. The reaction of **6** with XyNC in MeCN also took place at 60 °C, and from the resultant solution the monoisocyanide cluster $[(Cp^*Ir)_2(CpRu)(CNXy)\{\mu_3\text{-}SC(COOMe){=}CCOOMe\}(\mu_2\text{-}SCH_2CH_2CN)_2][PF_6]$ (**9b**) was isolated in 12% yield (eq 5). Another product present in the reaction mixture could not be isolated in a pure form, and its characterization was unsuccessful. Since the high-quality crystals were obtained for **9b**, the structure has been determined by X-ray analysis. An ORTEP drawing of the cation in **9b** is shown in Figure 5, while selected interatomic distances and angles are listed in Table 5.

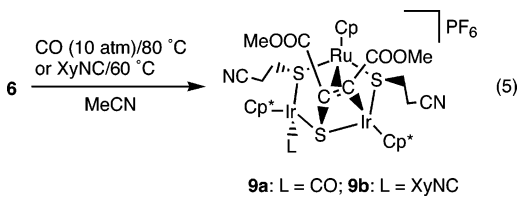

(5)

Cluster **9b** has a triangular core without any metal−metal bonding interactions. Two Ru−Ir edges are each bridged by the cyanoethylthiolato ligand, while the two

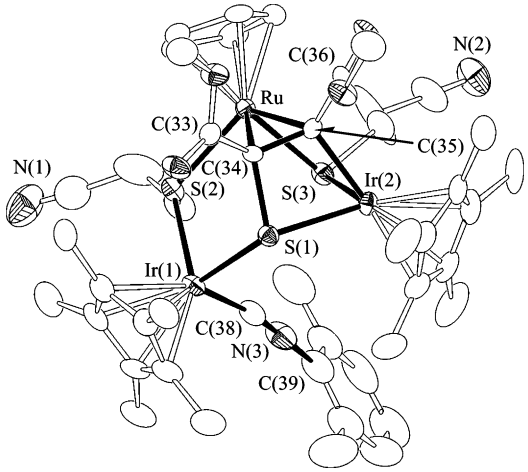

Figure 5. ORTEP drawing of the cation in **9b** at the 30% probability level. Hydrogen atoms are omitted for clarity.

Table 5. Selected Interatomic Distances (Å) and Angles (deg) in 9b

(a) Distances			
Ir(1)···Ru	4.0459(6)	Ir(1)···Ir(2)	4.1855(4)
Ir(2)···Ru	3.5108(7)		
Ir(1)−S(1)	2.342(2)	Ir(1)−S(2)	2.370(2)
Ir(1)−C(38)	1.930(8)	Ir(2)−S(1)	2.368(2)
Ir(2)−S(3)	2.359(2)	Ir(2)−C(35)	2.104(7)
Ru−S(2)	2.425(2)	Ru−S(3)	2.398(2)
Ru−C(34)	2.141(5)	Ru−C(35)	2.183(6)
S(1)−C(34)	1.833(7)	C(34)−C(35)	1.42(1)
N(3)−C(38)	1.15(1)		
(b) Angles			
S(1)−Ir(1)−S(2)	88.04(6)	S(1)−Ir(1)−C(38)	95.1(2)
S(2)−Ir(1)−C(38)	95.8(2)	S(1)−Ir(2)−S(3)	88.88(8)
S(1)−Ir(2)−C(35)	68.9(2)	S(3)−Ir(2)−C(35)	76.7(1)
S(2)−Ru−S(3)	85.20(7)		
Ir(1)−S(1)−Ir(2)	125.37(6)	Ir(1)−S(1)−C(34)	111.1(2)
Ir(2)−S(1)−C(34)	83.7(2)	Ir(1)−S(2)−Ru	115.10(7)
Ir(2)−S(3)−Ru	95.11(5)		
Ru−C(34)−S(1)	114.4(3)	Ru−C(34)−C(33)	118.0(5)
Ru−C(34)−C(35)	72.4(3)	S(1)−C(34)−C(33)	115.9(4)
S(1)−C(34)−C(35)	101.8(5)	C(33)−C(34)−C(35)	127.0(5)
Ir(2)−C(35)−Ru	110.0(2)	Ir(2)−C(35)−C(34)	105.2(4)
Ir(2)−C(35)−C(36)	117.4(5)	Ru−C(35)−C(34)	69.2(3)
Ru−C(35)−C(36)	121.5(4)	C(34)−C(35)−C(36)	124.0(5)
Ir(1)−C(38)−N(3)	170.4(7)	C(38)−N(3)−C(39)	176.0(9)

Ir atoms are connected by the S atom having its origin in the μ_3-S ligand in **4**. The DMAD molecule is now bound to one of these Ir−S bonds to yield a iridathiacyclobutene moiety, whose C=C bond is further ligating to the Ru atom. The isocyanide binds to the other coordinatively unsaturated Ir atom thus formed. One possible mechanism for converting **6** into **9** is illustrated in Scheme 3.

As expected, the iridathiacyclobutene ring is essentially planar with the torsion angle S(1)−Ir(2)−C(35)−C(34) of −4.8(4)°. The C(34)−C(35) distance of 1.42(1) Å is slightly shorter than the C−C bond length in the related ruthenathiacyclobutene complex [(Cp*Ru)$_2$(μ-S^{i}PrCH=CCOO^{t}Bu)(μ-S^{i}Pr)] (1.45(1) Å),[25] but considerably longer than those in the ferrathiacyclobutene complexes such as [Fe$_2$(CO)$_6$(μ-SCCF$_3$=CCF$_3$)] (1.406(5) Å)[24c] and [Fe$_2$(CO)$_6$(μ-SCPh=CH)] (1.379(6) Å)[23a] and the cluster with rhoda- and molybdathiacyclobutene units [{Rh(μ-SCPh=CH)Cl(PPh$_3$)}{Mo(μ-SCPh=CH)(S$_2$CNEt$_2$)}{Mo(S$_2$C$_2$PhH)(S$_2$CNEt$_2$)}] (1.39(1) and 1.37(1) Å).[22b] The two COOMe substituents are tilted from this IrSC$_2$ plane to the direction opposite the Ru atom with the angles of the C(33)−C(34) and C(36)−C(35) vectors toward the Ir(2)−S(1)−C(34)−C(35) least-squares plane at 38° and 43°, respectively. It is to be noted that although the metallathiacyclobutene moieties that are bonded further to the other metal in an η^2 or η^3 manner have been known for some time as cited here, those coordinating further to two more metals in η^2 and η^1 manners observed for **9** are unprecedented.

Scheme 3

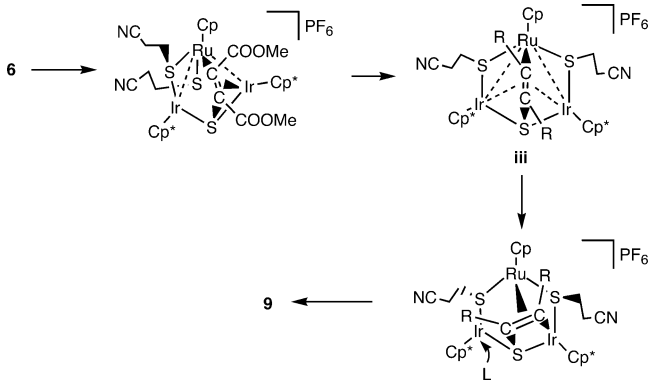

Experimental Section

General Procedures. All manipulations were performed under a nitrogen atmosphere using standard Schlenk techniques. Solvents were purified by common procedures. Complex **3**[10] and [CpRuCl(tmeda)][26] were prepared according to the literature methods, while other reagents were obtained commercially and used as received. The ^{1}H NMR spectra were recorded on a JEOL alpha-400 spectrometer, while the IR spectra were obtained from a JASCO FT/IR-420 spectrometer. Elemental analyses were done with a Perkin-Elmer 2400 series II CHN analyzer.

Preparation of [(Cp*Ir)$_2$(CpRu)Cl(μ_3-S)(μ_2-SCH$_2$CH$_2$CN)$_2$] (4). Complex **3** (218 mg, 0.254 mmol) and [CpRuCl(tmeda)] (84 mg, 0.26 mmol) dissolved in THF (20 mL) were stirred at room temperature for 24 h. The resultant dark red solution was dried in vacuo, and the residue was extracted with benzene. Addition of hexane to the concentrated extract gave dark red crystals of **4** (168 mg, 62% yield). ^{1}H NMR (C$_6$D$_6$): δ 1.46, 1.55 (s, 15H each, Cp*) 1.71−1.77 (m, 1H, CH$_2$), 1.91−2.04 (m, 3H, CH$_2$), 2.21 (dt, J = 16.8, 4.7 Hz, 1H, CH$_2$), 2.42−2.56 (m, 2H, CH$_2$), 3.60 (ddd, J = 11.2, 5.9, 4.7 Hz, 1H, CH$_2$), 4.18 (s, 5H, Cp). IR (KBr, cm^{-1}): ν(C≡N), 2245m. Anal. Calcd for C$_{31}$H$_{43}$ClIr$_2$N$_2$RuS$_3$: C, 35.10; H, 4.09; N, 2.64. Found: C, 35.41; H, 4.07; N, 2.37.

Preparation of [(Cp*Ir)$_2$(CpRu)(CO)(μ_3-S)(μ_2-SCH$_2$CH$_2$CN)$_2$][PF$_6$] (5a). A THF solution (5 mL) of **4** (52 mg, 0.049 mmol) and KPF$_6$ (16 mg, 0.087 mmol) was stirred under CO atmosphere (1 atm) at room temperature for 24 h. The resultant dark red suspension was dried, and the residue was crystallized from THF−hexane. Cluster **5a** was obtained as a dark brown solid (43 mg, 74% yield). ^{1}H NMR (CD$_3$CN): δ 1.75, 1.95 (s, 15H each, Cp*), 2.29 (ddd, 1H, J = 17.1, 8.5, 7.1 Hz, CH$_2$), 2.48 (ddd, 1H, J = 17.1, 6.8, 5.7 Hz, CH$_2$), 2.55−2.69 (m, 2H, CH$_2$), 2.82 (dt, 1H, J = 16.8, 6.1 Hz, CH$_2$), 2.88 (ddd, 1H, J = 12.9, 7.2, 5.7 Hz, CH$_2$), 3.10 (m, 1H, CH$_2$), 3.16 (ddd, 1H, J = 12.1, 8.2, 5.8 Hz, CH$_2$), 4.74 (s, 5H, Cp). IR (KBr, cm^{-1}): ν(C≡N), 2249m; ν(C≡O), 2021s. Anal. Calcd for C$_{32}$H$_{43}$F$_6$-

(25) Nishio, M.; Matsuzaka, H.; Mizobe, Y.; Tanase, T.; Hidai, M. *Organometallics* **1994**, *13*, 4214.

(26) (a) Trost, B. M.; Older, C. M. *Organometallics* **2002**, *21*, 2544. (b) Gemel, C.; Huffman, J. C.; Caulton, K. G.; Mauthner, K.; Kirchner, K. *J. Organomet. Chem.* **2000**, *593−594*, 342.

Table 6. Crystal Data for 4, 5b′, 6, 8, and 9b·THF

	4	5b′	6	8	9b·THF
formula	$C_{31}H_{43}ClIr_2N_2RuS_3$	$C_{64}H_{72}BIr_2N_3RuS_3$	$C_{37}H_{49}F_6Ir_2N_2O_4PRuS_3$	$C_{39}H_{56}F_6Ir_2NO_4PS_3Ru$	$C_{50}H_{66}F_6Ir_2N_3O_5PRuS$
fw	1060.84	1475.79	1312.46	1329.53	1515.74
space group	$P2_1/n$ (No. 14)	$P2/c$ (No. 13)	$P\bar{1}$ (No. 2)	$P\bar{1}$ (No. 2)	$P\bar{1}$ (No. 2)
a, Å	12.001(7)	19.233(3)	11.402(2)	13.080(6)	11.607(3)
b, Å	15.422(9)	11.069(2)	13.657(2)	13.435(6)	13.935(4)
c, Å	18.68(1)	28.768(5)	14.112(2)	15.430(9)	18.888(5)
α, deg	90	90	86.763(4)	73.06(2)	90.839(3)
β, deg	98.088(2)	103.8999(7)	77.398(4)	80.84(3)	105.421(3)
γ, deg	90	90	86.681(4)	59.36(2)	107.531(3)
V, Å^3	3423(4)	5945(2)	2138.9(5)	2231.6(19)	2793(1)
Z	4	4	2	2	2
ρ_{calcd}, g cm^{-3}	2.058	1.649	2.038	1.978	1.802
cryst size, mm^3	0.20 × 0.10 × 0.10	0.40 × 0.20 × 0.20	0.50 × 0.10 × 0.10	0.20 × 0.10 × 0.10	0.40 × 0.10 × 0.05
no. of unique reflns	7622	13556	9354	9742	12222
no. of data used	3593 ($I > 2\sigma(I)$)	8343 ($I > 2\sigma(I)$)	6945 ($I > 2\sigma(I)$)	6050 ($I > 2\sigma(I)$)	8227 ($I > 2\sigma(I)$)
no. of variables	399	739	554	569	675
transmn factor	0.252−0.428	0.233−0.377	0.273−0.505	0.293−0.520	0.503−0.770
R_1[a]	0.057	0.031	0.035	0.061	0.041
wR_2[b]	0.146	0.076	0.088	0.161	0.090
GOF[c]	1.025	1.023	1.036	1.033	1.046

[a] $R_1 = \sum||F_o| - |F_c||/\sum|F_o|$ ($I > 2\sigma(I)$). [b] $wR_2 = [\sum(w(F_o^2 - F_c^2)^2)/\sum w(F_o^2)^2]^{1/2}$ (all data). [c] GOF = $[\sum w(|F_o| - |F_c|)^2/\{$(no. observed) − (no. variables)$\}]^{1/2}$.

$Ir_2N_2OPRuS_3$: C, 32.07; H, 3.62; N, 2.34. Found: C, 32.08; H, 3.70; N, 2.16.

Preparation of [(Cp*Ir)$_2$(CpRu)(CNXy)(μ_3-S)(μ_2-SCH$_2$CH$_2$CN)$_2$][PF$_6$] (5b). A mixture of **4** (113 mg, 0.107 mmol), KPF_6 (30 mg, 0.16 mmol), and XyNC (16 mg, 0.12 mmol) in THF (10 mL) was stirred at room temperature for 24 h. The resultant dark brown suspension was dried, and the residue was crystallized from THF−MeCN−ether to give dark brown crystals of **5b**·MeCN (112 mg, 81% yield). ^{1}H NMR (CD_3CN): δ 1.73, 1.95 (s, 15H each, Cp*), 2.55 (s, 6H, Me), 2.43−2.51, 2.58−2.70, 2.79−2.88 (m, 2H each, CH_2), 2.29, 3.14 (m, 1H each, CH_2), 4.61 (s, 5H, Cp), 7.28−7.31 (m, 3H, C_6H_3). IR (KBr, cm^{-1}): ν(C≡N), 2249m; ν(N≡C) for XyNC, 2125s. Anal. Calcd for $C_{42}H_{55}F_6Ir_2N_4PRuS_3$: C, 37.57; H, 4.13; N, 4.17. Found: C, 37.60; H, 4.05; N, 3.94.

Preparation of [(Cp*Ir)$_2$(CpRu)(CNXy)(μ_3-S)(μ_2-SCH$_2$CH$_2$CN)$_2$][BPh$_4$] (5b′). This complex was prepared similarly from **4** (35 mg, 0.033 mmol), $NaBPh_4$ (15 mg, 0.044 mmol), and XyNC (5.7 mg, 0.043 mmol) in THF (4 mL). Crystallization of the product from CH_2Cl_2−hexane afforded **5b′** as dark brown crystals (12 mg, 25% yield). ^{1}H NMR (CD_3CN): δ 1.73, 1.95 (s, 15H each, Cp*), 2.55 (s, 6H, Me), 2.30 (dd, J = 16.6, 8.3 Hz, 1H, CH_2), 2.47 (ddd, J = 12.6, 7.2, 5.1 Hz, 1H, CH_2), 2.59 (dd, J = 12.2, 6.1 Hz, 1H, CH_2), 2.67 (ddd, J = 12.2, 10.0, 3.9 Hz, 1H, CH_2), 2.77−2.88 (m, 2H, CH_2), 2.96 (m, 1H, CH_2), 3.15 (ddd, J = 12.6, 10.3, 6.0 Hz, 1H, CH2), 4.61 (s, 5H, Cp), 6.83−7.30 (m, 23H, Ph and C_6H_3). IR (KBr, cm^{-1}): ν(C≡N), 2249m; ν(N≡C) for XyNC, 2128s. Anal. Calcd for $C_{64}H_{72}BIr_2N_3RuS_3$: C, 52.09; H, 4.92; N, 2.85. Found: C, 52.34; H, 4.98; N, 2.72.

Preparation of [(Cp*Ir)$_2$(CpRu){μ_3-SC(COOMe)=CCOOMe}(μ_2-SCH$_2$CH$_2$CN)$_2$][PF$_6$] (6). Into a THF solution (20 mL) of **4** (202 mg, 0.190 mmol) and KPF_6 (61 mg, 0.33 mmol) was added DMAD (93 mg, 0.65 mmol), and the mixture was stirred at room temperature for 12 h. The resultant red suspension was dried, and the residue was crystallized from MeCN−ether to give **6** as red crystals (174 mg, 70% yield). ^{1}H NMR (CD_3CN): δ 1.59 (m, 1H, CH_2), 1.76, 1.94 (s, 15H each, Cp*), 2.16−2.26 (m, 3H, CH_2), 2.51 (ddd, J = 17.3, 11.2, 5.1 Hz, 1H, CH_2), 2.78 (dt, J = 17.6, 5.0 Hz, 1H, CH_2), 2.90 (dt, J = 13.7, 5.0 Hz, 1H, CH_2), 3.16 (ddd, J = 13.4, 11.2, 5.0 Hz, 1H, CH_2), 3.71, 3.79 (s, 3H each, OMe), 5.01 (s, 5H, Cp). ^{13}C{^{1}H} NMR (CD_3CN): δ 70.6, 158.5 (C=C). IR (KBr, cm^{-1}): ν(C≡N), 2248m; ν(C=O), 1716s. Anal. Calcd for $C_{37}H_{49}F_6Ir_2N_2O_4PRuS_3$: C, 33.86; H, 3.76; N, 2.13. Found: C, 33.58; H, 3.66; N, 2.33.

Preparation of [(Cp*Ir)$_2$(Cp*Ru)(μ_3-S){μ_3-SC(COOMe)CHCOOMe}(μ_2-SCH$_2$CH$_2$CN)][PF$_6$] (8). Into a THF solution (20 mL) of **2**·1/2C_6H_6·1/2C_6H_{14} (122 mg, 0.101 mmol) and KPF_6 (30 mg, 0.16 mmol) was added DMAD (29 mg, 0.20 mmol), and the mixture was stirred at room temperature for 12 h. The resultant dark brown suspension was dried, and the residue was crystallized from MeCN−ether to give **8** as dark red crystals (53 mg, 40% yield). ^{1}H NMR (CD_3CN): δ 1.66, 1.73, 1.79 (s, 15H each, Cp*), 1.82 (m, 1H, CH_2), 2.66 (ddd, J = 15.2, 8.4, 6.8 Hz, 1H, CH_2), 2.73 (ddd, J = 12.6, 7.1, 5.6 Hz, 1H, CH_2), 3.75 (ddd, J = 12.5, 6.8, 5.6 Hz, 1H, CH_2), 3.45, 3.68 (s, 3H each, OMe), 4.25 (s, 1H, CH). ^{13}C NMR (CD_3CN): δ 50.6 (d, J_{C-H} = 139 Hz, SC−*C*H), 71.6 (S*C*−CH). IR (KBr, cm^{-1}): ν(C≡N), 2251m; ν(C=O), 1709s. Anal. Calcd for $C_{39}H_{56}F_6Ir_2NO_4PRuS_3$: C, 35.23; H, 4.25; N, 1.05. Found: C, 33.95; H, 4.11; N, 1.17.

Preparation of [(Cp*Ir)$_2$(CpRu)(CO){μ_3-SC(COOMe)=CCOOMe}(μ_2-SCH$_2$CH$_2$CN)$_2$] [PF$_6$] (9a). An acetonitrile solution (4 mL) of **6** (19 mg, 0.015 mmol) charged in a stainless autoclave was stirred under 10 atm of CO gas at 80 °C for 48 h. The color of the solution changed from red to orange during the reaction. The resultant solution was dried, and the residue was crystallized from CH_2Cl_2−ether to give **9a** as orange crystals (12 mg, 60% yield). ^{1}H NMR (CD_3CN): δ 1.61, 2.03 (s, 15H each, Cp*), 2.47 (ddd, J = 16.8, 9.0, 7.3 Hz, 1H, CH_2), 2.56−2.67 (m, 2H, CH_2), 2.74−2.84 (m, 2H, CH_2), 3.26−3.47 (m, 3H, CH_2), 3.49, 3.66 (s, 3H each, OMe), 5.44 (s, 5H, Cp). ^{13}C{^{1}H} NMR (CD_3CN): δ 72.4, 90.4 (C=C). IR (KBr, cm^{-1}): ν(C≡N), 2248m; ν(C≡O), 2027s; ν(C=O), 1685s. Anal. Calcd for $C_{38}H_{49}F_6Ir_2N_2O_5PRuS_3$: C, 34.05; H, 3.68; N, 2.09. Found: C, 34.08; H, 3.58; N, 2.35.

Preparation of [(Cp*Ir)$_2$(CpRu)(CNXy){μ_3-SC(COOMe)=CCOOMe}(μ_2-SCH$_2$CH$_2$CN)$_2$][PF$_6$] (9b). An acetonitrile solution (4 mL) of **6** (16 mg, 0.012 mmol) and XyNC (7.7 mg, 0.059 mmol) was stirred at 60 °C for 48 h. The color of the solution changed from red to yellow during the reaction. The resultant yellow solution was dried, and the residue was crystallized from MeCN−ether to give **9b**·MeCN as orange crystals (2.0 mg, 11% yield). ^{1}H NMR (CD_3CN): δ 1.44, 1.97 (s, 15H each, Cp*), 2.54 (s, 6H, Me), 2.56−2.74 (m, 3H, CH_2), 2.78 (ddd, J = 17.3, 7.8, 5.1 Hz, 1H, CH_2), 2.93 (ddd, J = 13.1, 8.5, 7.8 Hz, 1H, CH_2), 3.24 (ddd, J = 13.1, 8.6, 5.2 Hz, 1H, CH_2), 3.31 (dt, J = 13.0, 7.9 Hz, 1H, CH_2), 3.55 (m, 1H, CH_2), 3.47, 3.63 (s, 3H each, OMe), 4.83 (s, 5H, Cp), 7.19−7.29 (m, 3H, C_6H_3). ^{13}C{^{1}H} NMR (CD_3CN, δ): 81.4, 93.0 (C=C). IR (KBr, cm^{-1}): ν(C≡N), 2251m; ν(C≡N) for XyNC, 2126s; ν(C=O), 1687s. Anal. Calcd for $C_{48}H_{61}F_6Ir_2N_4O_4PRuS_3$: C, 38.83; H, 4.14; N, 3.77. Found: C, 38.90; H, 3.94; N, 3.79. Single crystals for the X-ray analysis have been grown from THF−ether.

X-ray Crystallography. The X-ray analyses of **4**, **5b′**, **6**, **8**, and **9b**·THF were carried out at room temperature on a

Rigaku Mercury-CCD diffractometer equipped with a graphite-monochromatized Mo Kα source. Details are listed in Table 6.

Structure solution and refinements were conducted by using the CrystalStructure program package.[27] The positions of non-hydrogen atoms were determined by Patterson methods (PATTY)[28] except for **8**, for which direct methods have been adopted (SHELX-97),[29] and subsequent Fourier synthesis (DIRDIF-99).[30] These were refined anisotropically except for those of solvating THF in **9b**, which were refined isotropically. For **8** and **9b**, disorders of PF_6 anions have been included in the calculations, where F atoms were refined isotropically. Hydrogen atoms other than H(53) in **8** were placed at the ideal positions and included at the final stages of refinements with fixed parameters, while the H(53) atom in **8** was found in the Fourier map and refined isotropically.

Acknowledgment. This work was supported by a Grant-in-Aid for Scientific Research on Priority Areas (No. 14078206, "Reaction Control of Dynamic Complexes") from the Ministry of Education, Culture, Sports, Science and Technology, Japan, and by CREST of JST (Japan Science and Technology Agency).

Supporting Information Available: Detailed results of X-ray crystallography for **4**, **5b′**, **6**, **8**, and **9b**·THF are available in CIF format free of charge via the Internet at http://pubs.acs.org.

OM050615A

(27) *CrystalStructure 3.00*: Crystal Structure Analysis Package; Rigaku and Rigaku/MSC, 2000−2002. Watkin, D. J.; Prout, C. K.; Carruthers, J. R.; Betteridge, P. W. *CRYSTALS Issue 10*; Chemical Crystallography Laboratory: Oxford, U.K.

(28) PATTY: Beurskens, P. T.; Admiraal, G.; Beurskens, G.; Bosman, W. P.; Garcia-Granda, S.; Gould, R. O.; Smits, J. M. M.; Smykall, C. *The DIRDIF Program System*; Technical Report of the Crystallography Laboratory; University of Nijmegen: Nijmegen, The Netherlands, 1992.

(29) SHELX-97: Sheldrick, G. M. *SHELX-97*, Program for the Refinement of Crystal Structures; University of Göttingen: Göttingen, Germany, 1997.

(30) DIRDIF-99: Beurskens, P. T.; Admiraal, G.; Beurskens, G.; Bosman, W. P.; de Gelder, R.; Israel, R.; Smits, J. M. M. *The DIRDIF-99 Program System*; Technical Report of the Crystallography Laboratory; University of Nijmegen: Nijmegen, The Netherlands, 1999.